Electronic Supplementary Information

Facet-Dependent Optical Properties of Polyhedral Au–Cu_2O Core–Shell Nanocrystals

Yu-Chen Yang,[†] Hsiang-Ju Wang,[‡] Jennifer Whang,[‡] Jer-Shing Huang,[‡] Lian-Ming Lyu,[‡] Po-Heng Lin,[‡] Shangjr Gwo,[†] and Michael H. Huang[*,‡]

[†]Department of Physics, National Tsing Hua University, Hsinchu 30013, Taiwan

[‡]Department of Chemistry, National Tsing Hua University, Hsinchu 30013, Taiwan

Synthesis of Octahedral Au Nanocrystals. The octahedral gold nanocrystal cores were synthesized following our reported hydrothermal synthesis procedure with slight modifications.[28] In a typical synthesis, 97 mL of deionized water, 0.55 g of CTAB surfactant, 2.5 mL of 0.01 M $HAuCl_4$ solution, and 0.5 mL of 0.1 M trisodium citrate solution were added to a home-made glass bottle with a volume capacity of 280 mL. The glass bottle was sealed by a Teflon bolt with an O-ring placed between the bottle and the Teflon cap. The bolt was fastened and wrapped with a polyimide tape to prevent the leakage of steam. Then the bottle was loaded into an oven set at 110 ºC. The reaction times were 12, 16, and 20 h to make Au octahedra with average sizes of 50, 60, and 70 nm, respectively. The particle size is defined as the opposite corner-to-corner distance as shown in Fig. 1 in the main text. After that, the bottle was removed from the oven and cooled naturally to room temperature. To collect the product, the solution was centrifuged at 6000 rpm for 20 min. The precipitate with a wine red color was drawn up by a micropipette and redispersed in deionized water with a total volume of 10 mL. This concentrated octahedral gold nanocrystal solution was kept at room temperature for future use. To remove the residual CTAB surfactant before using the Au nanocrystals as cores in the synthesis of Au–Cu_2O core–shell heterostructures, the concentrated octahedral gold nanocrystal solution was first centrifuged at 4000 rpm for 20 min. The supernatant was decanted and the precipitate was redispersed in the same volume of deionized water.

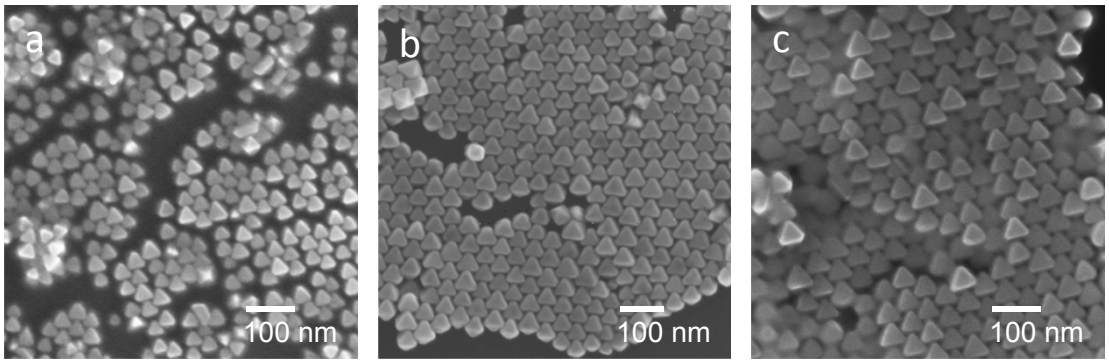

Fig. S1 (a–c) SEM images of the synthesized Au octahedra with sizes of (a) 50 ± 3 nm, (b) 60 ± 4 nm, and (c) 70 ± 4 nm. Particle size refers to opposite corner-to-corner distance. Standard deviation of particle sizes are (a) 6.5%, (b) 6.5 %, and (c) 5.6%.

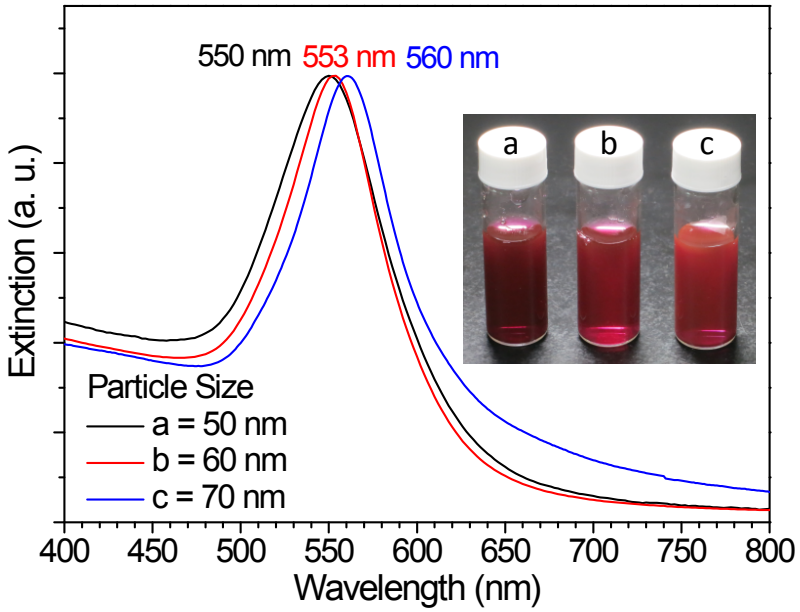

Fig. S2 UV–vis absorption spectra of the octahedral Au nanocrystal solutions. As average particle size increases from 50 nm to 70 nm, the band maximum shifts slightly from 550 nm to 560 nm. A photograph showing the particle solution colors is provided.

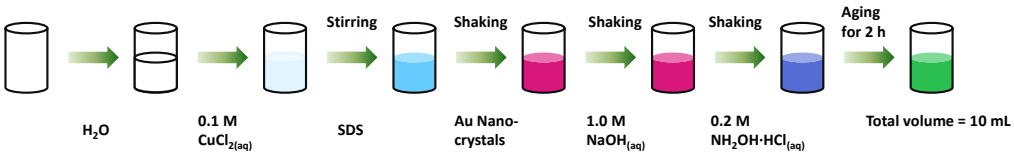

cubes	9.40 mL	0.1 mL	0.087 g	**0.05 mL**	0.25 mL	**0.20 mL**	Size = 182 nm
cuboctahedra	9.27 mL					**0.33 mL**	Size = 192 nm
octahedra	8.75 mL					**0.85 mL**	Size = 218 nm
cubes	9.35 mL	0.1 mL	0.087 g	**0.1 mL**	0.25 mL	**0.20 mL**	Size = 144 nm
cuboctahedra	9.22 mL					**0.33 mL**	Size = 162 nm
octahedra	8.70 mL					**0.85 mL**	Size = 187 nm
cubes	9.25 mL	0.1 mL	0.087 g	**0.2 mL**	0.25 mL	**0.20 mL**	Size = 113 nm
cuboctahedra	9.12 mL					**0.33 mL**	Size = 152 nm
octahedra	8.60 mL					**0.85 mL**	Size = 140 nm
cubes	9.15 mL	0.1 mL	0.087 g	**0.3 mL**	0.25 mL	**0.20 mL**	Size = 99 nm
cuboctahedra	9.02 mL					**0.33 mL**	Size = 131 nm
octahedra	8.50 mL					**0.85 mL**	Size = 122 nm
cubes	9.05 mL	0.1 mL	0.087 g	**0.4 mL**	0.25 mL	**0.20 mL**	Size = 92 nm
cuboctahedra	8.92 mL					**0.33 mL**	Size = 115 nm
octahedra	8.40 mL					**0.85 mL**	Size = 110 nm

Scheme S1 Schematic illustration of the synthetic procedure and the exact amounts of reagents used to make Au–Cu_2O core–shell nanocrystals. By increasing the volume of $NH_2OH{\cdot}HCl$ added, particle morphology can change from cubic to octahedral structure. By increasing the volume of concentrated octahedral Au nanocrystal solution introduced, smaller core–shell heterostructures were obtained. The volume of H_2O added was adjusted, such that the total solution volume was 10 mL.

Table S1 A list of the sizes of the synthesized Au–Cu_2O core–shell nanocrystals. Average particle sizes and their size distributions are provided. Narrow size distributions have been achieved for all samples, particularly for the cubes and cuboctahedra.

Cubes

Volume of Au core solution	Particle size	Standard deviation
0.05 mL	182 ± 8	4.4 %
0.1 mL	144 ± 6	4.2 %
0.2 mL	113 ± 6	4.5 %
0.3 mL	99 ± 6	6.1 %
0.4 mL	92 ± 6	6.5 %

Cuboctahedra

Volume of Au core solution	Particle size	Standard deviation
0.05 mL	192 ± 11	5.9 %
0.1 mL	162 ± 11	6.8 %
0.2 mL	152 ± 9	5.9 %
0.3 mL	131 ± 8	6.1 %
0.4 mL	115 ± 6	5.2 %

Octahedra

Volume of Au core solution	Particle size	Standard deviation
0.05 mL	218 ± 34 nm	15.6 %
0.1 mL	187 ± 23 nm	12.3 %
0.2 mL	140 ± 18 nm	12.9 %
0.3 mL	122 ± 14 nm	11.5 %
0.4 mL	110 ± 11 nm	10.0 %

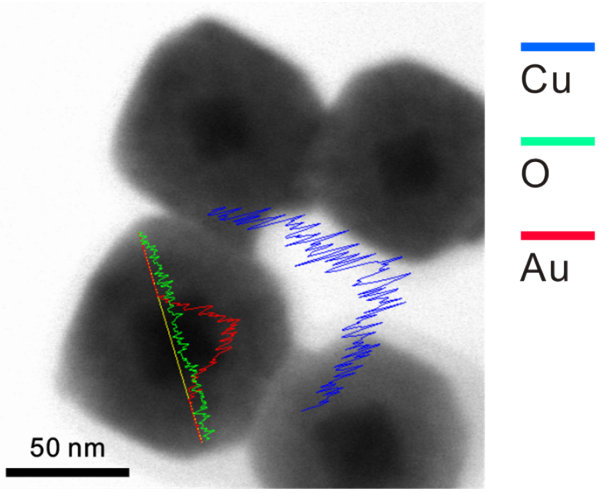

Fig. S3 EDS analysis of a single Au–Cu_2O core–shell cube. The EDS line-scan shows that Au is present only at the core of this particle.

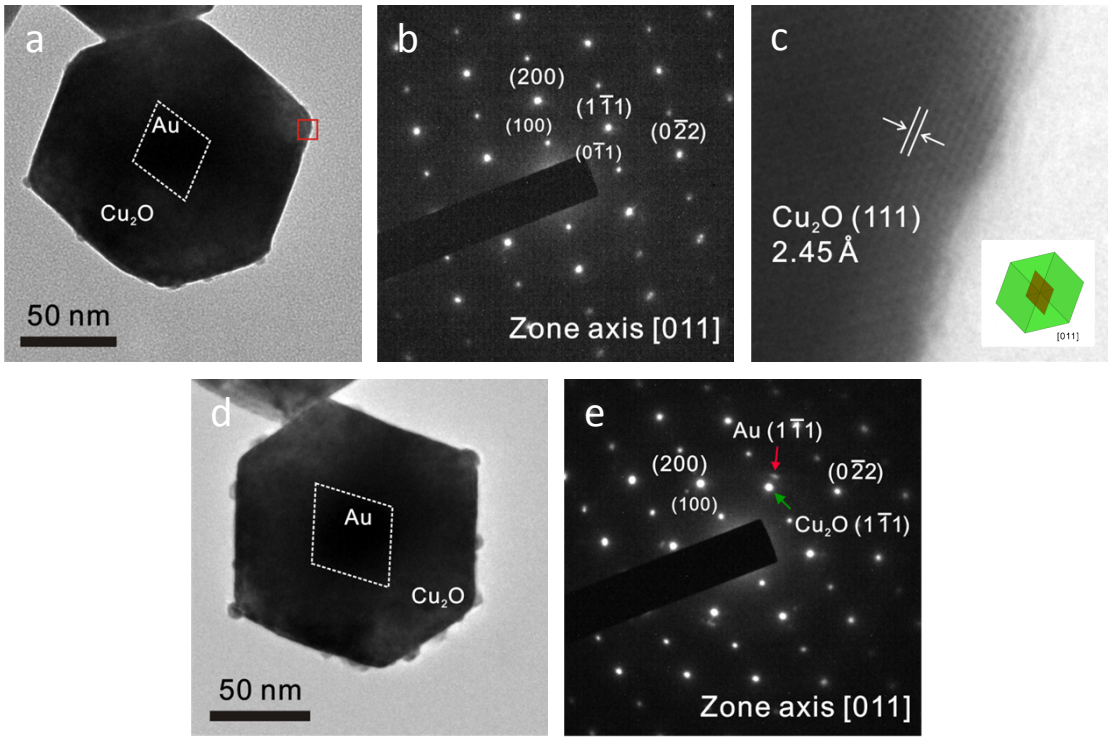

Fig. S4 TEM analysis of a single Au–Cu_2O core–shell cuboctahedron. (a) TEM image of a Au–Cu_2O cuboctahedron viewed along the [011] zone axis. Outline of the Au core is marked. (b) SAED pattern of this particle. (c) HR-TEM image of the red square region in (a). Cu_2O (111) lattice planes are measured. Inset gives a model of the particle viewed along the same direction as that shown in (a). (d and e) TEM image of another Au–Cu_2O cuboctahedron and its corresponding SAED pattern. Au diffraction spots can be seen, possibly due to a smaller particle size.

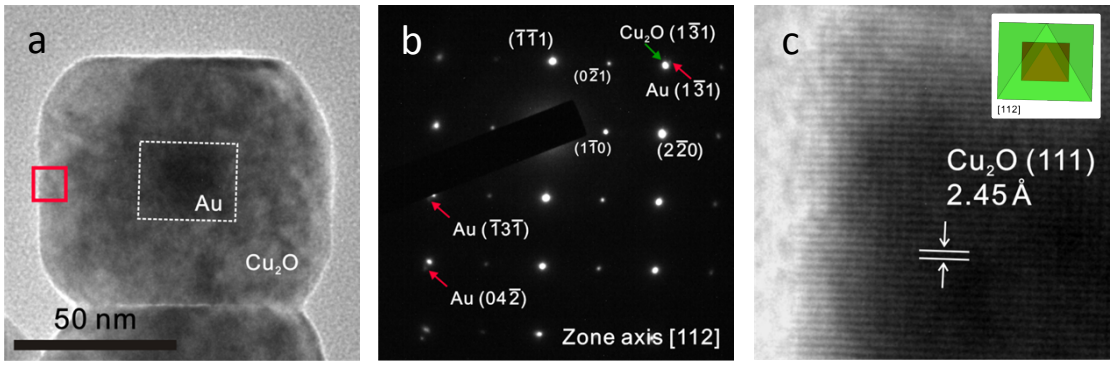

Fig. S5 (a and b) TEM image of a Au–Cu_2O core–shell octahedron viewed along the [112] direction and the corresponding SAED pattern. Both Au and Cu_2O diffraction spots are present. (c) HR-TEM image of the red square region in (a). Cu_2O (111) lattice planes are visible. The inset drawing has the same orientation as that of the particle in (a).

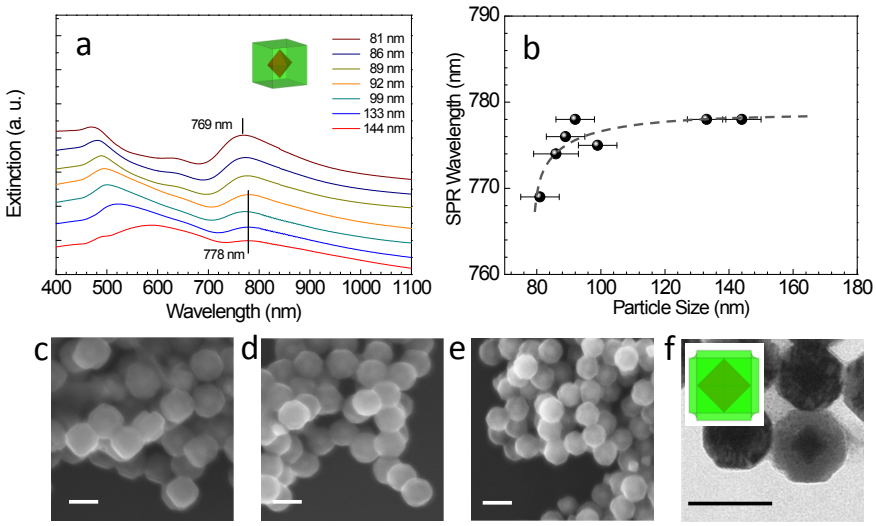

Fig. S6 UV–vis absorption spectra of the Au–Cu_2O core–shell nanocubes with 50-nm octahedral Au cores. (a) The UV–vis absorption spectra show that a spectral red shift of the Au SPR band from 769 nm to 778 nm occurs with increasing particle sizes. Particles with sizes beyond 86 nm show essentially a fixed SPR band position. (b) A plot showing the positions of the Au SPR band with respect to the particle size. The error bars give standard deviations of the particle sizes. The dash line is the best-fit line for the data points. (c, d and e) SEM images of the Au–Cu_2O nanocubes with sizes of (c) 89 nm, (d) 86 nm, and (e) 81 nm. Signifcant edge depressions make the nanocubes appear less cubic in appearance. The Au–Cu_2O nanocubes with sizes of 89, 86, 81 nm were synthesized by adding respectively 0.6, 0.8, and 1.2 mL of the concentrated octahedral Au nanocrystal solution to the reaction mixture. (f) TEM image of the 81-nm nanocubes. A schematic drawing is also provided. All scale bars are equal to 100 nm.

Table S2 Lists of the sizes of the synthesized Au–Cu_2O core–shell nanocrystals using 60-nm and 70-nm octahdral Au cores. Average particle sizes and their size distributions are provided.

Cubes

Volume of Au cores (60 nm) solution	Particle size	Standard deviation
0.05 mL	173 ± 12	7%
0.1 mL	158 ± 10	6%
0.2 mL	131 ± 9	7%
0.3 mL	117 ± 9	8%
0.4 mL	100 ± 7	7%

Octahedra

Volume of Au cores (60 nm) solution	Particle size	Standard deviation
0.05 mL	179 ± 26	15%
0.1 mL	148 ± 18	12%
0.2 mL	138 ± 15	11%
0.3 mL	126 ± 10	8%
0.4 mL	108 ± 10	9%

Cubes

Volume of Au cores (70 nm) solution	Particle size	Standard deviation
0.025 mL	207 ± 17	8 %
0.05 mL	175 ± 16	9 %
0.1 mL	146 ± 10	7 %
0.2 mL	135 ± 6	6 %
0.3 mL	124 ± 6	5 %
0.4 mL	116 ± 7	6 %
0.5 mL	108 ± 5	5 %

Octahedra

Volume of Au cores (70 nm) solution	Particle size	Standard deviation
0.025 mL	251 ± 13	5 %
0.05 mL	194 ± 16	8 %
0.1 mL	160 ± 8	5 %
0.2 mL	141 ± 8	6 %
0.3 mL	133 ± 6	4 %
0.4 mL	119 ± 7	6 %
0.5 mL	105 ± 6	6 %

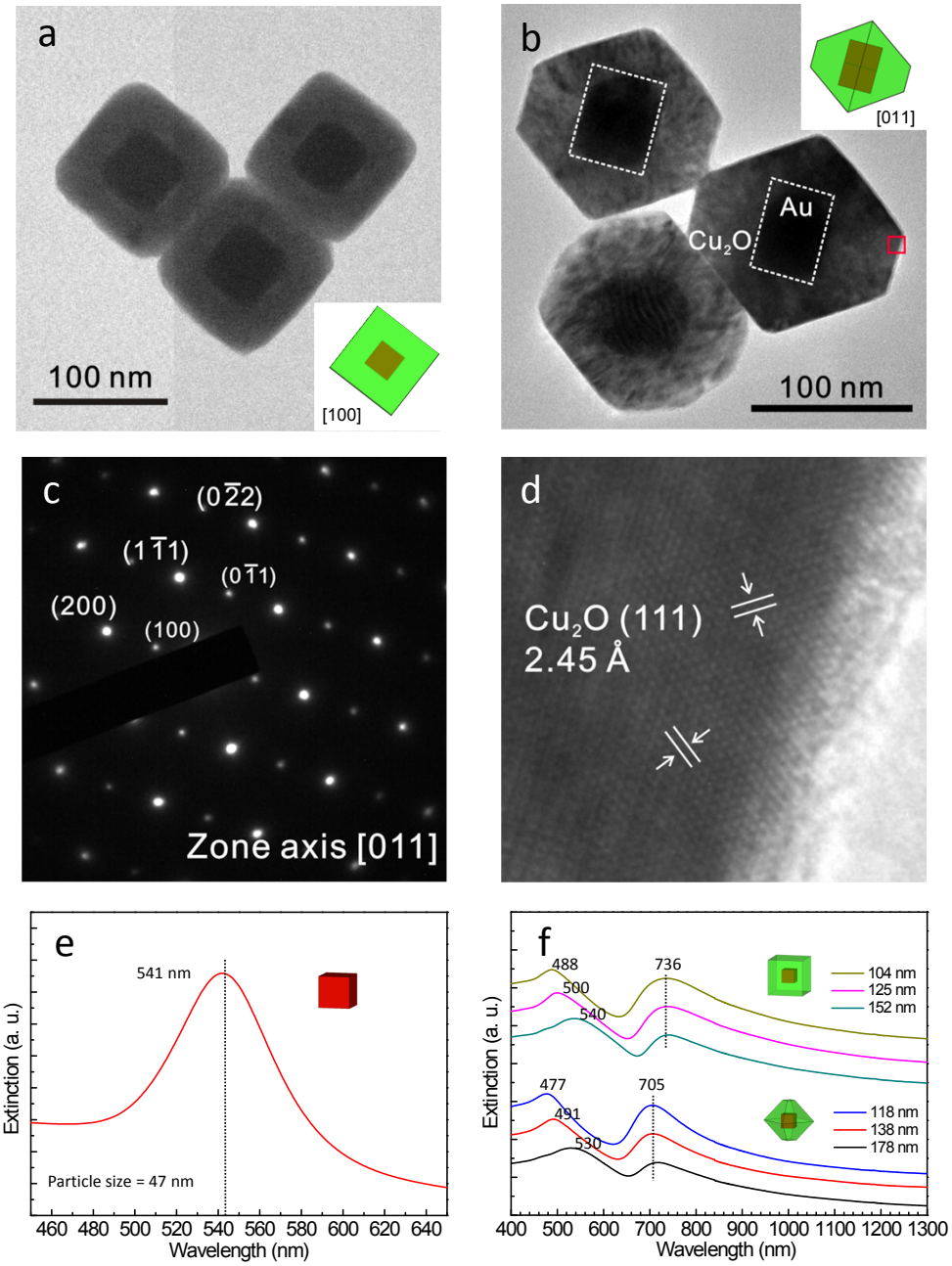

Fig. S7 TEM analysis and UV–vis absorption spectra of Au–Cu_2O core–shell nanocubes and truncated octahedra with 47-nm cubic Au cores. (a) TEM image of Au–Cu_2O core–shell cubes viewed from the [100] direction. Insets show a drawing of the particle having the same orientation. (b and c) TEM image of Au–Cu_2O core–shell truncated octahedra (b) and the corresponding SAED pattern of the right particle (c). The dotted lines give the outline of the cubic Au cores. Insets shows drawing of a core–shell truncated octahedron. (d) HR-TEM image of the red square region shown in (b). (e) UV–vis absorption spectrum of the cubic Au cores. (f) UV–vis absorption spectra of the Au–Cu_2O core–shell cubes and truncated octahedra with cubic Au cores. The Au SPR band position is fixed for each particle shape despite changes in the particle size.

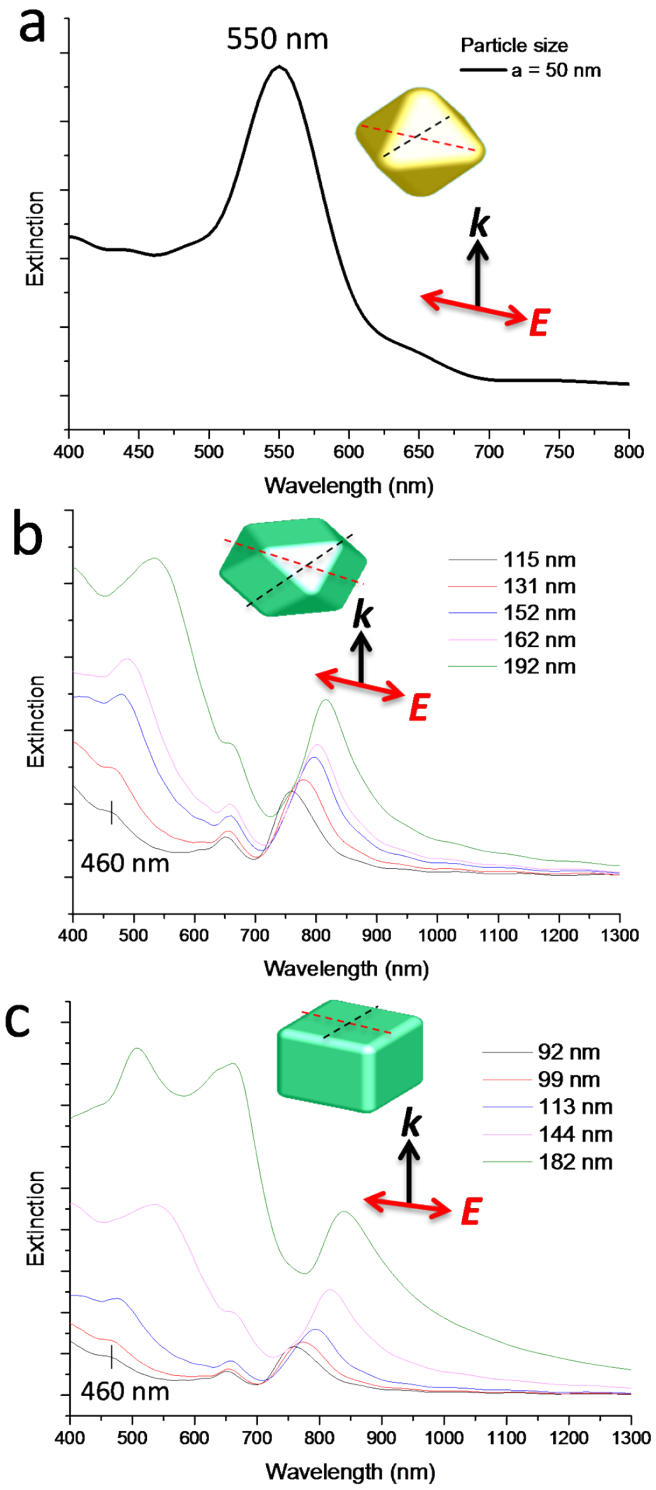

Fig. S8 (a) Normalized extinction spectrum of the bare octahedral cores. The polarization of the excitation plane wave is aligned to the diagonal of the octahedral cores. The inset shows the excitation geometry. (b and c) Simulation results for the UV–vis absorption spectra of (b) cuboctahedral and (c) cubic Au–Cu_2O core–shell nanocrystal solutions with different particle sizes.

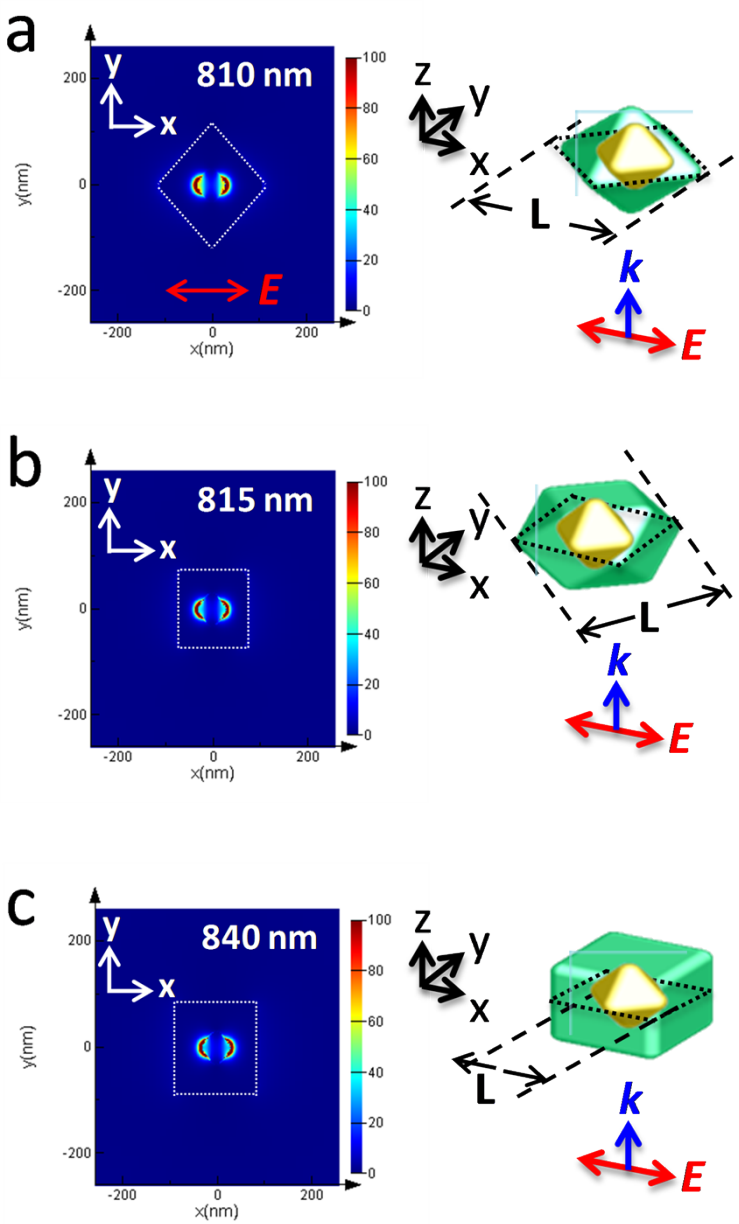

Fig. S9 Simulated electric near-field intensity distributions of Au–Cu_2O particles with (a) octahedral, (b) cuboctahedral, and (c) cubic shell with particle size **L** = 218, 192, and 182 nm, respectively. The enhancement distributions are recorded at the maximum in the extinction spectra at 810, 815, and 840 nm for the octahedral, cuboctahedral, and cubic shell, respectively. The excitation plane wave is linearly polarized along the diagonal of the octahedral core. The near-field distributions clearly show the dipolar resonance feature of the surface plasmon resonance of the gold core.

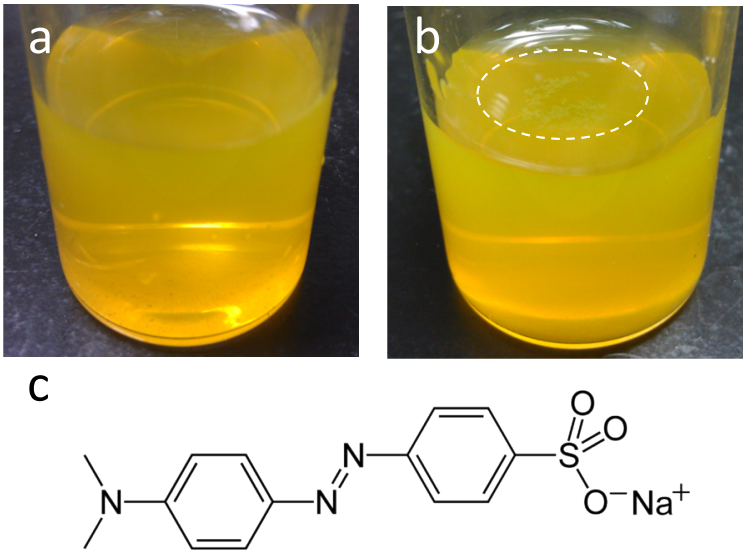

Fig. S10 Photograph of Au–Cu_2O core–shell octahedra and nanocubes dispersed in an aqueous methyl orange solution. (a) Octahedra can be well dispersed in this solution, but (b) nanocubes were found to float to the top of the solution after stirring. Electrostatic replusive interactions between the negative charged surfaces of the Au–Cu_2O core–shell nanocubes and anionic methyl orange may cause this phenomenon to appear. (c) Molecular structure of methyl orange.

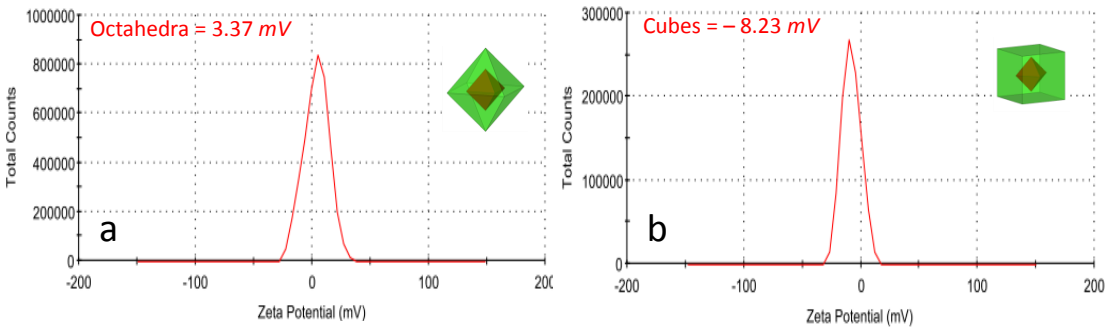

Fig. S11 Zeta potentials of the Au–Cu_2O core–shell octahedra and nanocubes. (a) Octahedra have a measured zeta potential value of 3.37 mV, while (b) nanocubes have a zeta potential value of –8.23 mV. The octahedra have an average size of 100 nm, while the nanocube have an average size of 90 nm. The Au core size is ~50 nm.

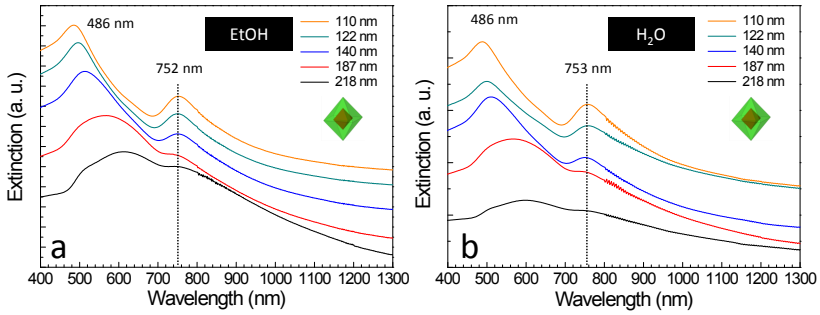

Fig. S12 (a and b) UV–vis absorption spectra of the Au–Cu_2O core–shell octahedra in ethanol and water. The spectra look almost identical for ethanol and water, because the two solutions have very close refractive indices.

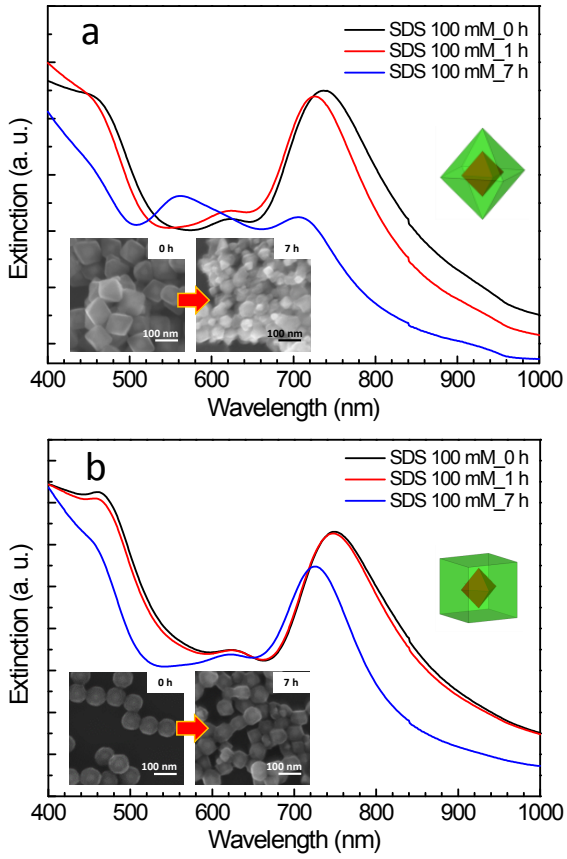

Fig. S13 UV–vis absorption spectra of (a) Au–Cu_2O core–shell octahedra and (b) cubes dispersed in water with 100 mM SDS for 0, 1, and 7 h. Here 0 h refers to spectra taken immediately after the nanocrystals were added to the SDS solution. Dramatic spectral blue shifts were observed after dispersing the nanocrystals in an aqueous solution with a high SDS concentration. The Cu_2O shells are largely destroyed after 7 h for the core–shell octahedra to expose the Au cores. The appearance of the 560 nm band from the Au cores and the corresponding SEM image of the resulting particles also indicate the exposure of the Au cores. The core–shell cubes were far more resistant to etching in the SDS solution.